

## RESEARCH ARTICLE

View Article Online

View Journal | View Issue

Cite this: *Org. Chem. Front.*, 2021, **8**, 2601

Received 14th December 2020,

Accepted 8th February 2021

DOI: 10.1039/d0qo01565b

rsc.li/frontiers-organic

Symmetric cytotoxic trimeric and dimeric indole alkaloids isolated from *Bousigonia angustifolia*†Bao-Bao Shi,<sup>a,b</sup> Jing-Song Lu,<sup>c</sup> Jing Wu,<sup>a,b</sup> Mei-Fen Bao<sup>a,b</sup> and Xiang-Hai Cai<sup>id</sup> <sup>\*,a</sup>

A symmetric monoterpenoid indole alkaloid trimer, bousangustine A, is reported for the first time, as well as the dimeric alkaloids bousangustines B and C; these were isolated from the trunks of *Bousigonia angustifolia*. The structures, which feature a symmetric 6/9/5/6 ring system, were elucidated using comprehensive spectroscopic analysis. Their absolute configurations were determined via X-ray crystal diffraction, as well as computational chemistry. They can be constructed through Friedel–Crafts and free radical reactions, respectively. These compounds exhibited significant cytotoxicity against tumor cells.

## Introduction

Since the development of bisindole vinblastine (VBL) and vincristine (VCR) into drugs, dimeric monoterpenoid indole alkaloids (MIAs) have attracted extensive attention. Owing to the inactive units of velbenamine and vindoline in VBL and VCR, the polymerization of indoles appears to be a crucial approach to obtain structural complexity, as well as bioactive diversity.<sup>1</sup> There are two forms of polymerization of MIAs (Fig. S1B in ESI†). One is through a direct connection, such as asymmetric voacandimine A,<sup>2</sup> coryzeylamine,<sup>3</sup> deformylcoryzeylamine,<sup>3</sup> suadimins A–C,<sup>4</sup> and symmetric geleganidine B.<sup>5</sup> The other is through an indirect connection, such as symmetric pleiokomenines A,<sup>6</sup> meloyines III,<sup>7</sup> melofusine I,<sup>8</sup> melomorsine I,<sup>8</sup> and voacinol<sup>2</sup> using methylene, as well as geleganidine C through a carbonyl.<sup>5</sup> Additionally, trimeric MIAs are unusual, for example, psychotripine from *Psychotria pilifera*,<sup>9</sup> ervadivamines A/B from *Ervatamia divaricata*,<sup>10</sup> and 3-hydroxy-14'-(3 $\alpha$ '-tabersonyl)voafrine B and 14-(3 $\alpha$ '-tabersonyl)-voafrine B in *Catharanthus roseus*,<sup>11</sup> bousigonine B in *Bousigonia mekongensis* have been previously reported.<sup>12</sup> These trimers are assembled by a single bond in sequence and are asymmetric structures. As part of our recent studies on dimeric<sup>7,8,13,14</sup> and trimeric alkaloids,<sup>15</sup> we have phytochemically researched plants of the genus *Bousigonia*, which contain bisindoles and

dimers.<sup>16</sup> This paper describes the isolation, structural determination, and potential bioactivity of three newly isolated MIAs (1–3) together with three known MIAs (4–6) (Fig. 1) obtained from the trunks of *B. angustifolia* Pierre.

## Results and discussion

Compounds 1–3 were obtained as an amorphous powder and exhibited a positive reaction to Dragendorff's reagent. The <sup>1</sup>H NMR spectrum of 1 revealed signals for four coupled indole protons ( $\delta_{\text{H}}$  7.10, 7.26, 7.18, 7.26), one olefinic proton ( $\delta_{\text{H}}$  5.06), one methyl ( $\delta_{\text{H}}$  0.60), one methine ( $\delta_{\text{H}}$  5.20, s), and six methylene protons ( $\delta_{\text{H}}$  1.39, 1.40, 1.80, 1.81, 2.07, 2.33, 2.34, each 1H, m;  $\delta_{\text{H}}$  1.38, 1H, d;  $\delta_{\text{H}}$  3.29 and 3.87, each 1H, dd;  $\delta_{\text{H}}$  1.67, 1H, td; and  $\delta_{\text{H}}$  1.13, 1H, dq) (Table 1). The 20 carbon signals in the <sup>13</sup>C NMR and DEPT spectra of 1 could be classified as seven quaternary carbons (including one carbonyl at  $\delta_{\text{C}}$  179.9 and five olefinic ones at  $\delta_{\text{C}}$  118.1, 131.1, 131.3, 139.5 and 141.6), six methines (including five olefinic ones at  $\delta_{\text{C}}$  111.1, 127.2, 127.9, 128.9 and 132.5), six methylenes ( $\delta_{\text{C}}$  20.3, 29.2, 31.1, 33.7, 37.9 and 44.4) and one methyl at  $\delta_{\text{C}}$  8.5 (Table 1). The molecular formula C<sub>58</sub>H<sub>64</sub>N<sub>6</sub>O<sub>3</sub> was established using the <sup>13</sup>C NMR and high-resolution electron ionization mass spectrometry (HREIMS) data ( $m/z$  915.4937 [M + Na]<sup>+</sup>, calculated for C<sub>58</sub>H<sub>64</sub>N<sub>6</sub>O<sub>3</sub>Na, 915.4932), which indicated 30 indices of hydrogen deficiency. However, the above described NMR data for 1 showed 20 carbon and 22 proton signals, only accounting for around one-third of the signals compared with the molecular formula. Therefore, compound 1 has a highly symmetrical structure. The planar structure was further elucidated by 2D NMR experiments. Analysis of the <sup>1</sup>H–<sup>1</sup>H correlation spectroscopy (COSY) and heteronuclear multiple quantum coherence (HMQC) spectra revealed the presence of three molecular fragments: fragment A (C<sub>3</sub>–C<sub>14</sub>–C<sub>15</sub>), fragment B (C<sub>16</sub>–C<sub>17</sub>),

<sup>a</sup>State Key Laboratory of Phytochemistry and Plant Resources in West China, Kunming Institute of Botany, Chinese Academy of Sciences, Kunming 650201, China. E-mail: xhcai@mail.kib.ac.cn

<sup>b</sup>University of Chinese Academy of Sciences, Beijing 100049, China

<sup>c</sup>Dongzhimen Hospital, Beijing University of Chinese Medicine, Beijing 100700, China

† Electronic supplementary information (ESI) available. CCDC 2048765. For ESI and crystallographic data in CIF or other electronic format see DOI: 10.1039/d0qo01565b



Fig. 1 Chemical structures of bousangustines A–C (1–3) and the known compounds 4–6.

Table 1  $^1\text{H}$  and  $^{13}\text{C}$  NMR spectroscopic data for 1–3 in methanol- $\text{d}_4$  ( $\delta$  in ppm and J in Hz)

| No.         | $\delta_{\text{C}}$ (1) <sup>b</sup> | $\delta_{\text{H}}$ (1) <sup>a</sup>       | $\delta_{\text{C}}$ (2) <sup>b</sup> | $\delta_{\text{H}}$ (2) <sup>a</sup>       | $\delta_{\text{C}}$ (3) <sup>c</sup> | $\delta_{\text{H}}$ (3) <sup>a</sup>       |
|-------------|--------------------------------------|--|--------------------------------------|--|--------------------------------------|--|
| 2/2'/2''    | 179.9 s                              |  | 180.1 s                              |  | 177.4 s                              |  |
| 3/3'/3''    | 44.4 t                               | 3.87 dd (12.4, 4.6)<br>3.29 dd (12.4, 4.0) | 44.4 t                               | 3.99 dd (12.2, 4.6)<br>3.50 td (12.2, 4.9) | 37.4 t                               | 4.19 d (13.7)<br>3.02 m                    |
| 5/5'/5''    | 131.1 s                              |  | 129.2 s                              |  | 165.8 s                              |  |
| 6/6'/6''    | 111.1 d                              | 5.06 s                                     | 110.1 d                              | 5.38 s                                     | 129.9 s                              |  |
| 7/7'/7''    | 118.1 s                              |  | 118.2 s                              |  | 154.5 s                              |  |
| 8/8'/8''    | 141.6 s                              |  | 141.6 s                              |  | 133.6 s                              |  |
| 9/9'/9''    | 132.5 d                              | 7.26 dd (7.7, 1.4)                         | 132.4 d                              | 7.36 dd (7.6, 1.7)                         | 130.3 d                              | 6.80 d (7.3)                               |
| 10/10'/10'' | 127.9 d                              | 7.18 td (7.7, 1.5)                         | 128.1 d                              | 7.28 td (7.6, 1.5)                         | 128.8 d                              | 6.80 t (7.3)                               |
| 11/11'/11'' | 128.9 d                              | 7.26 td (7.7, 1.4)                         | 128.9 d                              | 7.34 td (7.6, 1.7)                         | 130.4 d                              | 7.19 t (7.3)                               |
| 12/12'/12'' | 127.2 d                              | 7.10 dd (7.7, 1.5)                         | 127.4 d                              | 7.18 dd (7.6, 1.5)                         | 127.1 d                              | 7.00 d (7.3)                               |
| 13/13'/13'' | 139.5 s                              |  | 139.6 s                              |  | 135.3 s                              |  |
| 14/14'/14'' | 20.3 t                               | 2.07 m<br>1.81 m                           | 20.3 t                               | 2.15 m<br>1.90 m                           | 21.1 t                               | 1.55 m                                     |
| 15/15'/15'' | 33.7 t                               | 1.67 td (13.5, 3.1)<br>1.39 m              | 33.7 t                               | 1.72 td (13.5, 3.1)<br>1.46 m              | 34.5 t                               | 1.79 m<br>1.67 d (14.1)                    |
| 16/16'/16'' | 29.2 t                               | 2.34 m<br>1.80 m                           | 29.2 t                               | 2.40 m<br>1.86 t (7.8)                     | 28.2 t                               | 1.96 m                                     |
| 17/17'/17'' | 37.9 t                               | 2.33 m<br>1.40 m                           | 38.1 t                               | 2.40 m<br>1.46 m                           | 26.6 t                               | 1.79 m<br>1.52 t (4.6)                     |
| 18/18'/18'' | 8.5 q                                | 0.60 t (7.4)                               | 8.5 q                                | 0.69 t (7.3)                               | 7.5 q                                | 0.48 t (7.7)                               |
| 19/19'/19'' | 31.1 t                               | 1.13 dq (14.6, 7.4)<br>1.38 dq (14.6, 7.4) | 31.2 t                               | 1.19 dq (14.6, 7.3)<br>1.46 dq (14.6, 7.3) | 25.9 t                               | 1.04 dq (15.2, 7.7)<br>1.45 dq (15.2, 7.7) |
| 20/20'/20'' | 40.3 s                               |  | 40.2 s                               |  | 45.5 s                               |  |
| 21/21'/21'' | 131.3 s                              |  | 130.7 s                              |  | 93.8 s                               |  |
| 22          | 35.1 d                               | 5.20 s                                     | 25.0 t                               | 3.74 s                                     |                                      |  |

<sup>a</sup> Recorded at: 400 MHz. <sup>b</sup> Recorded at: 125 MHz. <sup>c</sup> Recorded at: 150 MHz.

fragment C (C<sub>18</sub>–C<sub>19</sub>) and an indole ring (Fig. 2). The hetero-nuclear multiple bond correlation (HMBC) correlations from H-3 to C-5 ( $\delta_{\text{C}}$  131.1) and C-21, from H-6 to C-7 ( $\delta_{\text{C}}$  118.1), C-8 ( $\delta_{\text{C}}$  141.6) and C-21, and from H-9 to C-7 indicated the presence of a pyrrole ring. Further analysis of the NMR spectrum suggested that **1** was closely related to known compounds **4** and **5**.<sup>17</sup> A careful comparison of the NMR data for **1** and **4** (Fig. S26 and S27†) disclosed the presence of an aldehyde group in **4**, and a methine ( $\delta_{\text{C}}$  35.1 and  $\delta_{\text{H}}$  5.20) appeared in **1**. The HMBC correlations from H-15 to C-17 ( $\delta_{\text{C}}$  37.9), C-19 ( $\delta_{\text{C}}$  31.1) and C-21 ( $\delta_{\text{C}}$  131.3), from H-19 to C-15 ( $\delta_{\text{C}}$  33.7), C-17 and C-21, and from H-17 to C-15, C-19 and C-21 further supported this similarity between **1** and **4**. The methine was connected with C-5 by the key HMBC correlations from its proton signal

$\delta_{\text{H}}$  5.20 to C-5 and C-6 ( $\delta_{\text{C}}$  111.1), and from H-6 ( $\delta_{\text{H}}$  5.06) to C-5, C-8, C-21 and its carbon signal ( $\delta_{\text{C}}$  35.1). Furthermore, taking the molecular formula into consideration, this methine should connect to another two of the same units. Thus, the complete planar structure of **1** was established.

The molecular formula C<sub>39</sub>H<sub>44</sub>N<sub>4</sub>O<sub>2</sub> with 20 degrees of unsaturation for alkaloid **2** was established by using the positive high resolution electrospray ionisation mass spectrometry (HRESIMS) ion at  $m/z$  623.3355 ([M + Na]<sup>+</sup>, calculated, 623.3356). The  $^{13}\text{C}$  NMR signals were only observed for 20 carbon atoms, indicating that **2** also has a symmetrical structure. The  $^1\text{H}$  and  $^{13}\text{C}$  NMR data of **2** were almost identical to those of compound **1** except for the methine group (CH-22) in **1**, there is a methylene group ( $\delta_{\text{C}}$  25.0) in **2** instead. This pre-



Fig. 2 Key HMBC and COSY correlations for compounds 1–3.

sumption was supported by the HMBC correlations from H-22 ( $\delta_{\text{H}}$  3.74, 2H) to C-5 ( $\delta_{\text{C}}$  129.2) and C-6 ( $\delta_{\text{C}}$  110.1), and from H-6 to C-5, C-21 ( $\delta_{\text{C}}$  130.7) and C-22 ( $\delta_{\text{C}}$  25.0). However, 2 had the molecular formula  $\text{C}_{39}\text{H}_{44}\text{N}_4\text{O}_2$  according to the results from the HRESIMS,  $\text{C}_{19}\text{H}_{20}\text{N}_2\text{O}$  less than compound 1. This difference suggests that 2 is a symmetric dimer of 4 through a methylene bridge. Therefore, the planar structure of 2 was completely established.

The molecular formula  $\text{C}_{38}\text{H}_{42}\text{N}_4\text{O}_6$  with 20 degrees of unsaturation of alkaloid 3 was established by the positive HRESIMS ion at  $m/z$  673.2992 ( $[\text{M} + \text{Na}]^+$ , calculated.

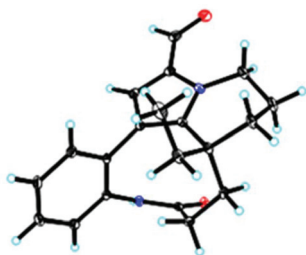


Fig. 3 The X-ray structure of compound 4.

673.2997). The NMR data (Table 1) showed signals for 19 carbons and 21 protons, only accounting for half the number expected from the molecular formula. This indicated that 3 should be a symmetric dimer. The  $^1\text{H}$  NMR spectrum also revealed the same indole A ring ( $\delta_{\text{H}}$  6.80, 7.00, 6.80, 7.19), one methyl ( $\delta_{\text{H}}$  0.48, 3H), and six methylene protons. The 19 carbon signals shown in the  $^{13}\text{C}$  NMR and DEPT spectra of 3 could be classified as eight quaternary carbons (including two carbonyls at  $\delta_{\text{C}}$  165.8 and 177.4; four olefinic ones at  $\delta_{\text{C}}$  129.9, 133.6, 135.3 and 154.5, and one heteroatom-bearing at  $\delta_{\text{C}}$  93.8), four indole methines ( $\delta_{\text{C}}$  127.1, 128.8, 130.3 and 130.4), six methylenes ( $\delta_{\text{C}}$  21.1, 25.9, 26.6, 28.2, 34.5 and 37.4), and one methyl ( $\delta_{\text{C}}$  7.5 q). The above described data for 1 was similar to that obtained for the known leuconolam (6),<sup>18</sup> except for the absence of the olefinic methine signal at  $\delta_{\text{C}}$  128.1 and the presence of a quaternary carbon signal at  $\delta_{\text{C}}$  129.9 in 1. For compound 3, the absence of a signal for H-6 ( $\delta_{\text{H}}$  5.79 in 6), together with the continuous correlations of H-9 ( $\delta_{\text{H}}$  6.80)/H-10 ( $\delta_{\text{H}}$  6.80)/H-11 ( $\delta_{\text{H}}$  7.19)/H-12 ( $\delta_{\text{H}}$  7.00) in the COSY spectrum (Fig. 2), indicated that both units must be directly connected through C-6/C-6'.

Unfortunately, attempts to prepare single crystals of 1–3 were not successful. However, a single crystal of alkaloid 4,

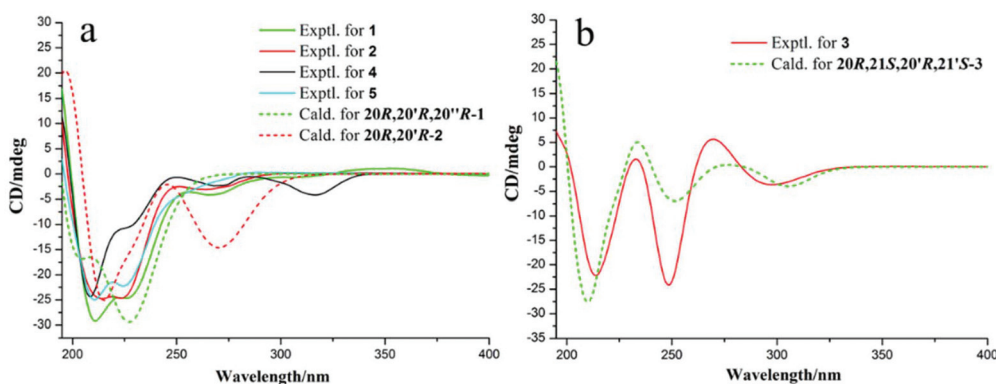
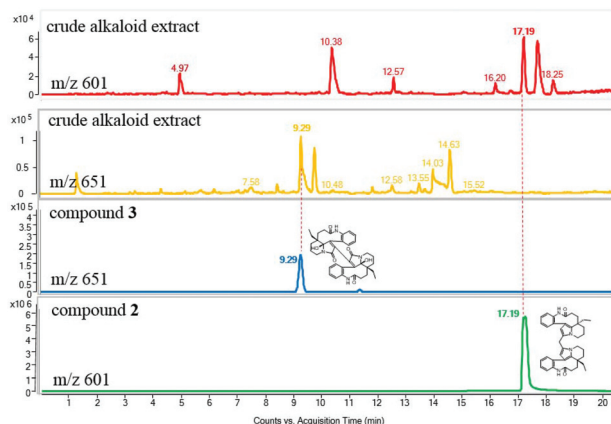


Fig. 4 (a) Experimental ECD spectra and calculated ECD spectra for 1–2 and 4–5; and (b) experimental ECD spectra and calculated ECD spectra of 3 at the M06-2X/Def2SVP level in methanol.

and units of **1** and **2**, were obtained. The X-ray diffraction analysis with Cu K $\alpha$  radiation resulted in a Flack parameter of  $-0.01(6)$ , giving the absolute configuration of alkaloid **4** (Fig. 3) as *20R*. With regards to the biogenetic relationship between **1**, **2**, **4** and **5**, the stereochemical structures of the four



**Fig. 5** Positive-ion mode LC-MS analysis of the crude alkaloid extract and polymeric alkaloids (extracted ion chromatograms at *m/z* 601 and 651; conditions: YMC-pack ODS-A C<sub>18</sub>: 4.6 × 150 mm, flow rate: 1 mL min<sup>-1</sup>, a linear gradient of 10–100% CH<sub>3</sub>CN containing 0.01% NH<sub>4</sub>OH over 20 min, then eluting with 100% CH<sub>3</sub>CN for an additional 10 min).

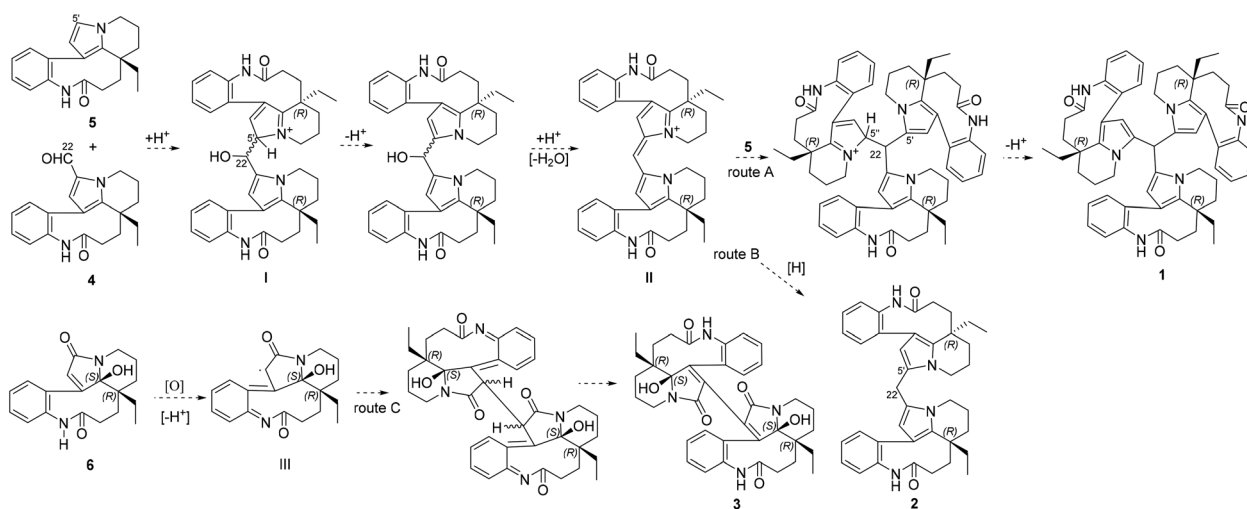
**Table 2** *In vitro* cytotoxic activities of **1–6** (IC<sub>50</sub> ± SD in μM)

| No.         | SMMC-7721    | HeLa         | HepG2       | A549         |
|-------------|--------------|--------------|-------------|--------------|
| <b>1</b>    | 10.99 ± 0.34 | 12.50 ± 1.11 | 16.3 ± 0.15 | 16.93 ± 0.33 |
| <b>2</b>    | 4.31 ± 0.06  | 4.40 ± 0.30  | 7.02 ± 0.55 | 16.21 ± 0.01 |
| <b>3</b>    | >40          | >40          | >40         | >40          |
| <b>4</b>    | 0.52 ± 0.04  | 0.60 ± 0.03  | 0.76 ± 0.05 | >40          |
| <b>5</b>    | 1.89 ± 0.22  | 1.76 ± 0.02  | 3.46 ± 0.22 | >40          |
| <b>6</b>    | >40          | >40          | >40         | >40          |
| Vinorelbine | 3.02 ± 0.21  | 0.60 ± 0.03  | 0.76 ± 0.05 | 2.23 ± 0.06  |

compounds were predicted to be identical. Therefore, the absolute configurations of **1** and **2** were determined to be *20R,20'R,20''R* and *20R,20'R*, respectively. Furthermore, the calculated electronic circular dichroism (ECD) spectra were used to support this prediction. Although the Cotton effects of **1** and **2** were stronger and slightly shifted compared to those observed for **4** and **5** (Fig. 4a), the tendencies of the CD curves of the four compounds in the range of 200 to 350 nm were relatively consistent, supporting their identical configurations. In addition, the identity of the measured CD and calculated ECD spectrum of **1** and **2** (Fig. 4a) further confirmed this conclusion. Similar to **1** and **2**, **4** and **5**, **3** and **6** were predicted to have the same absolute configurations. A further search of the previously published literature revealed leuconolam as an authentic sample of a natural product, and its structure was unambiguously determined using X-ray analysis.<sup>18</sup> Further comparison of the experimental chemical shifts and the calculated and experimental ECD spectra of **6** (Table S5 and Fig. S43†) revealed that **6** was leuconolam. Therefore, the stereoconfiguration of **3** was temporarily deduced as *20R,21S,20'R,21'S*. This assumption was confirmed by comparative analysis of the calculated and experimental ECD spectra. The identity of the measured circular dichroism (CD) and the calculated ECD spectra of **3** (Fig. 4b) supported this prediction. It should be mentioned that compound **3** possessed fast axial rotation rates in the order of seconds or faster and exhibited no axial chirality based on the correlation of the calculated energy barriers and rotation rates ( $\Delta E_{\text{rot}} < 20 \text{ kcal mol}^{-1}$ ) (Fig. S42†).<sup>19</sup>

To determine whether the compounds occurred naturally *in vivo*, an UPLC-MS/MS analysis was performed. The dimeric alkaloids **2–3** could be detected as trace compounds in the total alkaloid fraction, which means that these alkaloids were probably natural products (Fig. 5).

All of the isolates were evaluated *in vitro* against SMMC-7721, HeLa, HepG2, and A549 tumor cell lines.



**Scheme 1** Proposed pathways to the dimeric and trimeric MIAs.



Compound **4** exhibited significant cytotoxicity against the SMMC-7721, HeLa and HepG2 cell lines with  $IC_{50}$  values of  $0.52 \pm 0.04$ ,  $0.60 \pm 0.03$  and  $0.76 \pm 0.05$   $\mu\text{M}$ , respectively. Compounds **1** and **2** showed moderate cytotoxic activities against SMMC-7721, HeLa, HepG2, and A549 cells, with  $IC_{50}$  values ranging from 4.31 to 16.93  $\mu\text{M}$ . Compounds **3** and **6** showed no cytotoxicity at 40  $\mu\text{M}$  (Table 2).

Bousangustines A–C (**1**–**3**) are novel symmetrical MIAs trimer and dimers. Together with these, three known MIAs, rhazinal (**4**), rhazinilam (**5**), and leuconolam (**6**), were simultaneously isolated. Hence, we propose a plausible biosynthetic pathway for alkaloids **1**–**3** (Scheme 1). The pathway for **1**–**2** could start from **4** and **5** through a Friedel–Crafts reaction under acid conditions, generating the hydroxy intermediate I. I is then dehydrated to produce intermediate II. II is further coupled with **5**, forming trimer **1** (Scheme 1, route A). On the other hand, II is reduced and gives dimer **2** (route B). Unlike the formation of **1** and **2**, **6** is oxidized to generate the free radical intermediate III. The coupling of both units III gives **3** after isomerization (route C).

## Conclusions

In summary, three previously unreported bousangustines A–C were isolated from *B. angustifolia*. Bousangustine A is the first reported symmetric MIA trimer and bousangustines B–C are symmetric dimeric MIAs. Their absolute configurations were determined using X-ray crystal diffraction and ECD calculations. Bousangustines A and B may be constructed through a Friedel–Crafts reaction, while bousangustine C could be formed through free radical coupling from simultaneously isolated monomers. The liquid chromatography mass spectrometry (LC-MS) detection results of these novel isolates disclosed their natural properties. Furthermore, these macrocyclic compounds exhibited excellent cytotoxic activities. These findings enrich our knowledge of the chemical diversity of MIAs and will attract the interest of both chemical synthetic and pharmaceutical chemists.

## Experimental section

### General experimental procedures

The optical rotations were measured using a Jasco P-1020 digital polarimeter (Jasco International Co., Tokyo, Japan). UV spectra were recorded on a Shimadzu 2401PC spectrophotometer (Shimadzu Corp., Kyoto, Japan). CD spectra were obtained on a Chirascan V100 circular dichroism spectrometer (Applied Photophysics, Surrey, UK). The MS data were recorded on an UPLC-IT-TOF MS (Shimadzu Corp., Kyoto, Japan) or Agilent G6230 TOF MS (Applied Biosystems, Ltd, Warrington, UK).  $^1\text{H}$ ,  $^{13}\text{C}$  and 2D NMR spectra were obtained on Bruker AVANCE III-600, AVANCE III-500 and AVANCE III-400 MHz spectrometers (Bruker BioSpin GmbH, Rheinstetten, Germany) with  $\text{SiMe}_4$  as an internal standard. The chemical shifts ( $\delta$ ) are

expressed in ppm with reference to the solvent signals. X-ray crystallographic analysis using Cu K $\alpha$  radiation was performed on a Bruker D8 QUEST instrument (Bruker, Karlsruhe, Germany). Column chromatography (CC) was performed on either silica gel (200–300 mesh, Qingdao Marine Chemical Co., Ltd, Qingdao, China) or RP-18 silica gel (20–45  $\mu\text{m}$ , Fuji Silysia Chemical Ltd, Japan). Fractions were monitored by TLC on silica gel plates (GF254, Qingdao Marine Chemical Co., Ltd, Qingdao, China), and spots were visualized with Dragendorff's reagent spray. Medium pressure liquid chromatography (MPLC) was performed using a Buchi pump system coupled with RP-18 silica gel-packed glass columns (15  $\times$  230 and 26  $\times$  460 mm, respectively). High performance liquid chromatography (HPLC) was performed using Waters 1525E pumps (Waters Corp., Milford, MA, USA) coupled with analytical semi-preparative or preparative XBridge  $\text{C}_{18}$  columns (4.6  $\times$  150, 10  $\times$  150, and 19  $\times$  250 mm, respectively). The HPLC system employed a Waters 2998 photodiode array detector and a Waters fraction collector III (Waters Corp., Milford, MA, USA).

### Plant material

Trunks of *Bousigonia angustifolia* Pierre were collected in Dec 2018 in areas along the Mengla County, Yunnan Province, P. R. China, and identified by Dr Jie Cai. A voucher specimen (No. Cai20181228) was deposited in the State Key Laboratory of Phytochemistry and Plant Resources in West China, Kunming Institute of Botany, Chinese Academy of Sciences.

### Extraction and separation

The dried and powdered trunks of *B. angustifolia* (25 kg) were extracted with MeOH (60 L  $\times$  3) at room temperature, these were then filtered and the solvent was evaporated *in vacuo*. The extract was dissolved in 0.5% aqueous HCl solution and extracted with ethyl acetate (EtOAc) three times. The remaining acidic aqueous solution was basified with 10%  $\text{NH}_4\text{OH}$  to pH 7–8, and subsequently extracted with EtOAc. This afforded 210 g of the crude alkaloidal fraction. This EtOAc extract (210 g) was subjected to column chromatography (CC) over silica gel and eluted with gradient  $\text{CHCl}_3$ –MeOH (1 : 0–0 : 1, v/v) to afford ten fractions (I–X). Fraction I (17.4 g) was chromatographed on a  $\text{C}_{18}$  MPLC column eluted with a gradient of MeOH– $\text{H}_2\text{O}$  (10 : 90–100 : 0, v/v) to give the eighteen subfractions I-1–I-18. Fraction I-12 (2.2g) was separated using a Sephadex LH-20 column eluted with MeOH. Six subfractions (I-12-1–I-12-6) were collected. I-12-6 (0.4 g) was separated using a  $\text{C}_{18}$  MPLC column with a gradient of MeOH– $\text{H}_2\text{O}$  (60 : 40–90 : 10, v/v) to afford three subfractions (I-12-6-1–I-12-6-3). Fraction I-12-6-1 (0.11 g) was purified using a preparative  $\text{C}_{18}$  HPLC column with a gradient of MeCN– $\text{H}_2\text{O}$  (30 : 70–45 : 55, v/v) to obtain **5** (12.5 mg, 33.5 min). Fraction I-12-6-2 (0.15 g) was purified using a preparative  $\text{C}_{18}$  HPLC column with a gradient of MeCN– $\text{H}_2\text{O}$  (40 : 60–55 : 45, v/v) to obtain **1** (2.4 mg, 69.3 min), **2** (9.1 mg, 50.2min) and **4** (9.8 mg, 27.4 min). Fraction I-18 (1.1g) was separated using a Sephadex LH-20 column eluted with MeOH. Five subfractions (I-18-1–I-18-5) were collected. Fraction I-18-3 (0.12g) was purified

using a preparative C<sub>18</sub> HPLC column with a gradient of MeCN–H<sub>2</sub>O (40 : 60–55 : 45, v/v) to obtain **3** (9.1 mg, 34.8 min). Fraction II (21.5 g) was chromatographed on a C<sub>18</sub> MPLC column eluted with a gradient of MeOH–H<sub>2</sub>O (10 : 90–100 : 0, v/v) to give the twelve subfractions II-1–II-12. Fraction II-7 (3.3g) was separated using a Sephadex LH-20 column eluted with MeOH. Eight subfractions (II-7-1–II-7-8) were collected. Fraction II-7-7 (0.09 g) was purified using a preparative C<sub>18</sub> HPLC column with a gradient of MeCN–H<sub>2</sub>O (25 : 75–40 : 60, v/v) to obtain **6** (8.7 mg, 24.6 min).

**Bousangustine A (1):** yellowish amorphous powder; C<sub>58</sub>H<sub>64</sub>N<sub>6</sub>O<sub>3</sub>; [ $\alpha$ ]<sub>D</sub><sup>23</sup> –669.3 (c, 0.10, CH<sub>3</sub>OH); UV (CH<sub>3</sub>OH)  $\lambda_{\max}$  (log  $\epsilon$ ) 195 (4.20), 348 (2.96) nm; <sup>1</sup>H (400 MHz) and <sup>13</sup>C (125 MHz) NMR data (methanol-*d*<sub>4</sub>) (Table 1); positive ESIMS *m/z* 915 [M + Na]<sup>+</sup>. HRESIMS (*m/z* 915.4937 [M + Na]<sup>+</sup>, calculated for C<sub>58</sub>H<sub>64</sub>N<sub>6</sub>O<sub>3</sub>Na 915.4932).

**Bousangustine B (2):** yellowish amorphous powder; C<sub>39</sub>H<sub>44</sub>N<sub>4</sub>O<sub>2</sub>; [ $\alpha$ ]<sub>D</sub><sup>23</sup> –347.84 (c, 0.14, CH<sub>3</sub>OH); UV (CH<sub>3</sub>OH)  $\lambda_{\max}$  (log  $\epsilon$ ) 195 (4.24) nm; <sup>1</sup>H (400 MHz) and <sup>13</sup>C (125 MHz) NMR data (methanol-*d*<sub>4</sub>) (Table 1); positive ESIMS *m/z* 623 [M + Na]<sup>+</sup>. HRESIMS (*m/z* 623.3355 [M + Na]<sup>+</sup>, calculated for C<sub>39</sub>H<sub>44</sub>N<sub>4</sub>O<sub>2</sub>Na 623.3356).

**Bousangustine C (3):** yellowish amorphous powder; C<sub>38</sub>H<sub>42</sub>N<sub>4</sub>O<sub>6</sub>; [ $\alpha$ ]<sub>D</sub><sup>23</sup> –201.5 (c, 0.08, CH<sub>3</sub>OH); UV (CH<sub>3</sub>OH)  $\lambda_{\max}$  (log  $\epsilon$ ) 195 (3.81) nm; <sup>1</sup>H (400 MHz) and <sup>13</sup>C (150 MHz) NMR data (methanol-*d*<sub>4</sub>) (Table 1); positive ESIMS *m/z* 673 [M + Na]<sup>+</sup>. HRESIMS (*m/z* 673.2992 [M + Na]<sup>+</sup>, calculated for C<sub>38</sub>H<sub>42</sub>N<sub>4</sub>O<sub>6</sub>Na 673.2997).

### Bioassays

The cytotoxicity of compounds **1–6** was tested using the MTS assay. The cells were seeded into 96-well tissue culture dishes at 4 × 10<sup>3</sup> cells per well for HeLa and 5 × 10<sup>3</sup> cells per well for SMMC-7721, HepG2, and A-549 and cultured overnight at 37 °C in a 5% CO<sub>2</sub> incubator for cell adhesion. Cells were then incubated in culture medium with each compound for 48 h. The MTS-reducing activity was evaluated by measuring the absorbance at 490 nm using a Cell Titer 96 A Queous One Solution Cell Proliferation Assay kit (Promega, USA) and an Infinite M200 Pro (Tecan, Austria) microplate reader. IC<sub>50</sub> values were calculated using the Reed–Muench method.

## Conflicts of interest

There are no conflicts to declare.

## Acknowledgements

This project was supported in part by the Applied Basic Research Key Project of Yunnan (No. 2016FA030) and the National Natural Science Foundation of China (31872677). Computational resources used in this work were supported in part by SciGrid, Chinese Academy of Sciences.

## Notes and references

- 1 A. Keglevich, A. Szigetvari, M. Dekany, C. Szantay, P. Keglevich and L. Hazai, Synthesis and in vitro antitumor effect of new vindoline Derivatives Coupled with triphenylphosphine, *Curr. Org. Chem.*, 2019, **23**, 852–858.
- 2 M. Kitajima, M. Iwai, N. Kogure, R. Kikura-Hanajiri, Y. Goda and H. Takayama, Aspidosperma-aspidosperma-type bisindole alkaloids from Voacanga africana, *Tetrahedron*, 2013, **69**, 796–801.
- 3 H. Takayama, S. Subhadhirasakul, J. Mizuki, M. Kitajima, N. Aimi, D. Ponglux and S. Sakai, A new class of two dimeric indole alkaloids, coryzeylamine and deformylcoryzeylamine, from the leaves of Hunteria zeylanica in Thailand, *Chem. Pharm. Bull.*, 1994, **42**, 1957–1959.
- 4 X. H. Gao, Y. Y. Fan, Q. F. Liu, S. H. Cho, G. F. Pauli, S. N. Chen and J. M. Yue, Suadimins A–C, unprecedented dimeric quinoline alkaloids with antimycobacterial activity from Melodinus suaveolens, *Org. Lett.*, 2019, **21**, 7065–7068.
- 5 W. Zhang, X. J. Huang, S. Y. Zhang, D. M. Zhang, R. W. Jiang, J. Y. Hu, X. Q. Zhang, L. Wang and W. C. Ye, Geleganidines A–C, unusual monoterpenoid indole alkaloids from Gelsemium elegans, *J. Nat. Prod.*, 2015, **78**, 2036–2044.
- 6 E. O. N. Obiang, G. Genta-Jouve, J. F. Gallard, B. Kumulungui, E. Mouray, P. Grellier, L. Evanno, E. Poupon, P. Champy and M. A. Beniddir, Pleiokomenines A and B: dimeric aspidofractinine alkaloids tethered with a methylene group, *Org. Lett.*, 2017, **19**, 6180–6183.
- 7 B. J. Zhang, C. Liu, M. F. Bao, X. H. Zhong, L. Ni, J. Wu and X. H. Cai, Novel monoterpenoid indole alkaloids from Melodinus yunnanensis, *Tetrahedron*, 2017, **73**, 5821–5826.
- 8 X. H. Cai, H. Jiang, Y. Li, G. G. Cheng, Y. P. Liu, T. Feng and X. D. Luo, Cytotoxic indole alkaloids from Melodinus fusiformis and M. morsei, *Chin. J. Nat. Med.*, 2011, **9**, 259–263.
- 9 X. N. Li, Y. Zhang, X. H. Cai, T. Feng, Y. P. Liu, Y. Li, J. Ren, H. J. Zhu and X. D. Luo, Psychotripine: a new trimeric pyrrolindoline derivative from Psychotria pilifera, *Org. Lett.*, 2011, **13**, 5896–5899.
- 10 Z. W. Liu, J. Zhang, S. T. Li, M. Q. Liu, X. J. Huang, Y. L. Ao, C. L. Fan, D. M. Zhang, Q. W. Zhang, W. C. Ye and X. Q. Zhang, Ervadivamines A and B, two unusual trimeric monoterpenoid indole alkaloids from Ervatamia divaricata, *J. Org. Chem.*, 2018, **83**, 10613–10618.
- 11 H. Schubel, W. Fahn and J. Stockigt, Formation of the first trimeric monoterpenoid indole alkaloids, *Helv. Chim. Acta*, 1989, **72**, 147–150.
- 12 Y. L. Wang, C. R. Guo, Y. Mu, Y. L. Lin, H. J. Yan, Z. W. Wang and X. J. Wang, Bousigonine A and B, bis- and tri-indole alkaloids from Bousigonia mekongensis and their preventing high glucose-induced podocyte injury activity, *Tetrahedron Lett.*, 2019, **60**, 151042.
- 13 B. J. Zhang, B. Wu, M. F. Bao, L. Ni and X. H. Cai, New dimeric and trimeric Erythrina alkaloids from Erythrina variegata, *RSC Adv.*, 2016, **6**, 87863–87868.

- 14 Y. Yu, S. M. Zhao, M. F. Bao and X. H. Cai, Aspidosperma-type alkaloid dimer from *Tabernaemontana bovina* as a candidate for inhibition of microglial activation, *Org. Chem. Front.*, 2020, **11**, 1365–1373.
- 15 B. J. Zhang, M. F. Bao, C. X. Zeng, X. H. Zhong, L. Ni, Y. Zeng and X. H. Cai, Dimeric Erythrina alkaloids from the flower of *Erythrina variegata*, *Org. Lett.*, 2014, **16**, 6400–6403.
- 16 (a) Y. H. Fu, H. P. He, Y. T. Di, S. L. Li, Y. Zhang and X. J. Hao, Mekongenines A and B, two new alkaloids from *Bousigonia mekongensis*, *Tetrahedron Lett.*, 2012, **53**, 3642–3646; (b) Y. H. Fu, S. L. Li, S. F. Li, H. P. He, Y. T. Di, Y. Zhang and X. J. Hao, Cytotoxic eburnamine-aspidospermine type bisindole alkaloids from *Bousigonia mekongensis*, *Fitoterapia*, 2014, **98**, 45–52; (c) Y. H. Fu, Y. T. Di, H. P. He, S. L. Li, Y. Zhang and X. J. Hao, Angustifonines A and B, cytotoxic bisindole alkaloids from *Bousigonia angustifolia*, *J. Nat. Prod.*, 2014, **77**, 57–62.
- 17 T. S. Kam, Y. M. Tee and G. Subramaniam, Rhazinal, a formylrhazinilam derivative from a Malayan *Kopsia*, *Nat. Prod. Lett.*, 1998, **12**, 307–310.
- 18 S. H. Goh, A. R. M. Ali and W. H. Wong, Alkaloids of *Leuconotis griffithii* and *L. eugenifolia* (Apocynaceae), *Tetrahedron*, 1989, **45**, 7899–7902.
- 19 S. R. LaPlante, P. J. Edwards, L. D. Fader, A. Jakalian and O. Hucke, Revealing atropisomer axial chirality in drug discovery, *ChemMedChem*, 2011, **6**, 505–513.